

583  
NPS-PH-92-003

# NAVAL POSTGRADUATE SCHOOL

## Monterey, California



ANNUAL SUMMARY OF BASIC RESEARCH  
IN THERMOACOUSTIC HEAT TRANSPORT: 1991

ANTHONY A. ATCHLEY

OCTOBER 1991

Technical Report

Approved for public release; distribution unlimited.

Prepared for:  
Office of Naval Research  
Washington, VA 22217-5000

FEDDOCS  
D 208.14/2  
NPS-PH-92-003

NAVAL POSTGRADUATE SCHOOL  
MONTEREY, CALIFORNIA

Rear Admiral R. W. West, Jr.  
Superintendent

H. Shull  
Provost

This report was prepared for and funded by the Office of Naval Research, Physics Division,  
Code 1112, 800 North Quincy Street, Arlington, VA., 22217-5000.

This report was prepared by:

# REPORT DOCUMENTATION PAGE

Form Approved  
NAVAL POSTGRADUATE SCHOOL  
MONTEREY CA 93943-5000  
OMB No. 0704-0188/101

Public reporting burden for this collection of information is estimated to average 1 hour per response, including the time for reviewing instructions, searching existing data sources, gathering and maintaining the data needed, and completing and reviewing the collection of information. Send comments regarding this burden estimate or any other aspect of this collection of information, including suggestions for reducing this burden, to Washington Headquarters Services, Directorate for Information Operations and Reports, 1215 Jefferson Davis Highway, Suite 1204, Arlington, VA 22202-4302, and to the Office of Management and Budget, Paperwork Reduction Project (0704-0188), Washington, DC 20503.

1. AGENCY USE ONLY (Leave blank)		2. REPORT DATE 28 Oct 91	3. REPORT TYPE AND DATES COVERED Summary 01 Oct 90 - 30 Sep 91	
4. TITLE AND SUBTITLE  ANNUAL SUMMARY OF BASIC RESEARCH IN THERMOACOUSTIC HEAT TRANSPORT: 1991			5. FUNDING NUMBERS  PE 61153N G N0001491WR24003 TA 4126949	
6. AUTHOR(S)  ANTHONY A. ATCHLEY				
7. PERFORMING ORGANIZATION NAME(S) AND ADDRESS(ES) Physics Department Naval Postgraduate School Monterey, CA 93943-5000			8. PERFORMING ORGANIZATION REPORT NUMBER  NPS-PH-92-003	
9. SPONSORING/MONITORING AGENCY NAME(S) AND ADDRESS(ES) Office of Naval Research Physics Division-Code 1112 800 North Quincy Street Arlington, VA 22217-5000			10. SPONSORING/MONITORING AGENCY REPORT NUMBER	
11. SUPPLEMENTARY NOTES				
12a. DISTRIBUTION /AVAILABILITY STATEMENT  Approved for public release: Distribution unlimited.			12b. DISTRIBUTION CODE	
13. ABSTRACT (Maximum 200 words) This annual report details progress in basic research in thermoacoustic heat transport made during the period October 1, 1990 through September 30, 1991. Five projects are discussed: an experimental study of edge effects in thermoacoustic couple measurements, the application of porous media techniques to thermoacoustic prime movers, development of a non-boundary layer, non-short stack model for the power output of a thermoacoustic prime mover, the study of the transition to steady state oscillation in a thermoacoustic prime mover above onset of self-oscillation, and the study of energy distribution and dissipation in finite amplitude standing waves. A publications, patents, presentations, and honors report is also included.				
14. SUBJECT TERMS  Thermoacoustics, prime movers, heat transport, standing waves, nonlinear acoustics.			15. NUMBER OF PAGES 35	
			16. PRICE CODE	
17. SECURITY CLASSIFICATION OF REPORT  UNCLASSIFIED	18. SECURITY CLASSIFICATION OF THIS PAGE  UNCLASSIFIED	19. SECURITY CLASSIFICATION OF ABSTRACT  UNCLASSIFIED	20. LIMITATION OF ABSTRACT	



## ABSTRACT

This annual report details progress in basic research in thermoacoustic heat transport made during the period October 1, 1990 through September 30, 1991. Five projects are discussed: an experimental study of edge effects in thermoacoustic couple measurements, the application of porous media techniques to thermoacoustic prime movers, development of a non-boundary layer, non-short stack model for the power output of a thermoacoustic prime mover, the study of the transition to steady state oscillation in a thermoacoustic prime mover above onset of self-oscillation, and the study of energy distribution and dissipation in finite amplitude standing waves. A publications, patents, presentations, and honors report is also included.

## SUMMARY OF PROGRESS

The long term goal of this research is to develop a thorough understanding of thermoacoustic phenomena. During FY 1991, our investigations concentrated on five areas: an experimental study of edge effects in thermoacoustic couple measurements, the application of porous media techniques to thermoacoustic prime movers, development of a non-boundary layer, non-short stack model for the power output of a thermoacoustic prime mover, the study of the transition to steady state oscillation in a thermoacoustic prime mover above onset of self-oscillation, and the study of energy distribution and dissipation in finite amplitude standing waves. The first two projects straddled FYs 1990 and 1991. The remaining three were initiated in FY 1991. A brief discussion of these investigations is given in this report.

### 1. Experimental Study of Edge Effects in Thermoacoustic Couple Measurements

In previous years we devoted a large effort to measuring the temperature difference developed across a simple class of thermoacoustic engine, called a thermoacoustic couple or TAC. The results of these extensive measurements are discussed in detail in Ref. 1. To summarize the findings, large discrepancies between the predicted and measured temperature differences appear at high acoustic amplitudes. Although the reason(s) for these discrepancies is (are) unknown, some possible explanations are suggested in Ref. 1. One possibility involves the TAC design. The temperature difference was measured with a series of thermocouples (called a thermopile) placed along the front and back edges of the TAC. Because of its proximity to the edge, the thermopile may be sensitive to effects that, though perhaps causing *local* deviations in the temperature profile, do not affect the



temperature profile in interior regions of the plate. In other words, although considerable deviations are observed between theory and measurements made at the plate edges, the interior (and majority) of the plate may behave according to predictions.

To investigate whether edge effects are the cause of the discrepancies, we have constructed a TAC with two thermopiles, whose junctions do not lie along the edge, and made the same type of measurements as described in Ref. 1. These measurements are discussed in detail in Refs. 2 and 3. The results show that the temperature profile in the interior of the TAC behaves the same as that measured at the edge. Therefore, the irregularities previously observed are not an artifact of placing the thermopile along the edge. The irregularities may still be the result of the edge (e.g., turbulence generated at the edge), but they are not isolated at the edge. They extend at least half way to the center of the TAC.

Although the cause of the discrepancy between theory and measurement is still unknown, the number of possibilities has at least been reduced. Of the remaining possible causes, turbulence and acoustic streaming are the most probable candidates.

## 2. Application of Porous Media Techniques to Thermoacoustic Prime Movers

In FY 1990, we began to investigate thermoacoustic prime movers below the onset of self-oscillation. The quality factor  $Q$  of a helium filled prime mover was determined from measurements of its frequency response. Measurements were made for mean pressures ranging from 170 - 500 kPa and temperature differences across the stack ranging from zero to that required for onset of self-oscillation. As the temperature difference is increased, the  $Q$  increases indicating a decrease in attenuation across the stack. Analysis of the data and refinements to the theory continued in FY 1991 as discussed below, which is a summary of a complete

discussion presented in Ref. 4.

The results of the measurements are explained in terms of a counterpropagating, plane wave analysis, based on techniques commonly used in porous media investigations. The results of the calculations are shown in Figs 1-3, along with the experimental data. These figures show graphs of  $1/Q$ , which is proportional to the net attenuation in the prime mover, versus temperature difference. The figures correspond to mean gas pressures of 170, 376, and 500 kPa, respectively. The individual symbols represent the measurements and the lines show the results of the calculations. The agreement between the theory and experiment at the two higher pressures is very good. There are some noticeable differences at the lowest pressure. The theory over predicts the attenuation at low temperature differences and under predicts the onset temperature ( $1/Q = 0$ ).

Measurements were also made for the second and third longitudinal modes of the prime mover at a mean gas pressure of 170 kPa. The data and calculations are shown in Fig. 4. The  $\times$ 's and solid line correspond to the second mode, while the open squares and dashed line correspond to the third. It was not possible to make measurements near onset for these modes, because the onset temperatures exceed that of the fundamental. The overall agreement is good. The tendency to over predict the attenuation at zero temperature difference decreases. No conclusions can be drawn concerning the ability to predict the onset temperature.

The theory presented in Ref. 4 is intended only to be approximate in that it does not consider the complications of the temperature dependence of thermophysical properties of the prime mover components in a detailed manner. However, it does show that a counterpropagating wave analysis, commonly used in porous media research, does offer a relatively good explanation of the data. Collaborators at the University of Mississippi, have developed a more thorough theoretical development<sup>5</sup> and have used our data to verify it.<sup>6</sup>



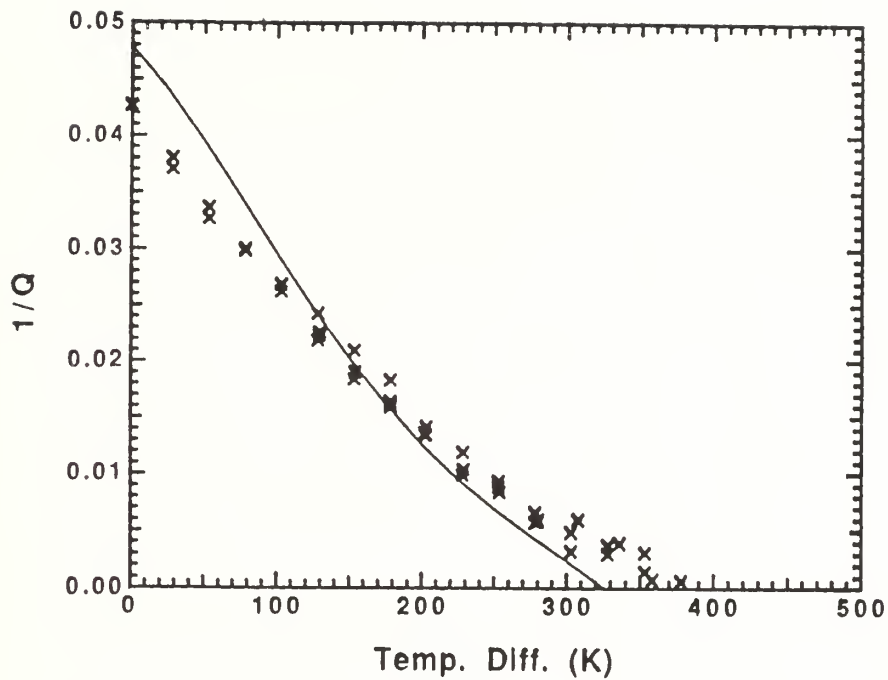


Figure 1. Graph of  $1/Q$  vs the temperature difference across the prime mover stack. The symbols represent the data, while the line represents the results of the calculations. The prime mover is filled with helium at a mean pressure of 170 kPa.

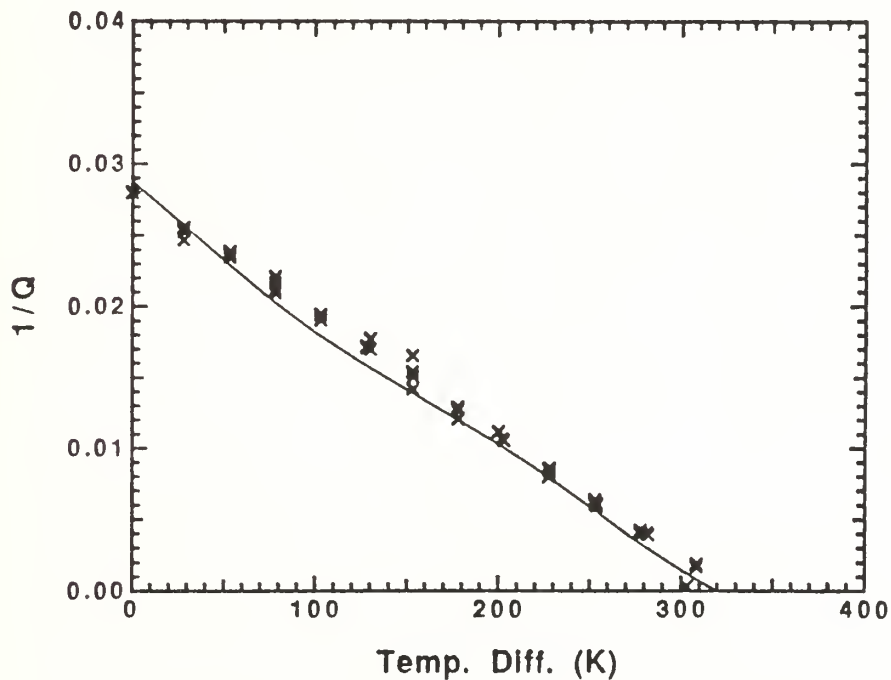


Figure 2. Graph of  $1/Q$  vs the temperature difference across the prime mover stack. The symbols represent the data, while the line represents the results of the calculations. The prime mover is filled with helium at a mean pressure of 376 kPa.

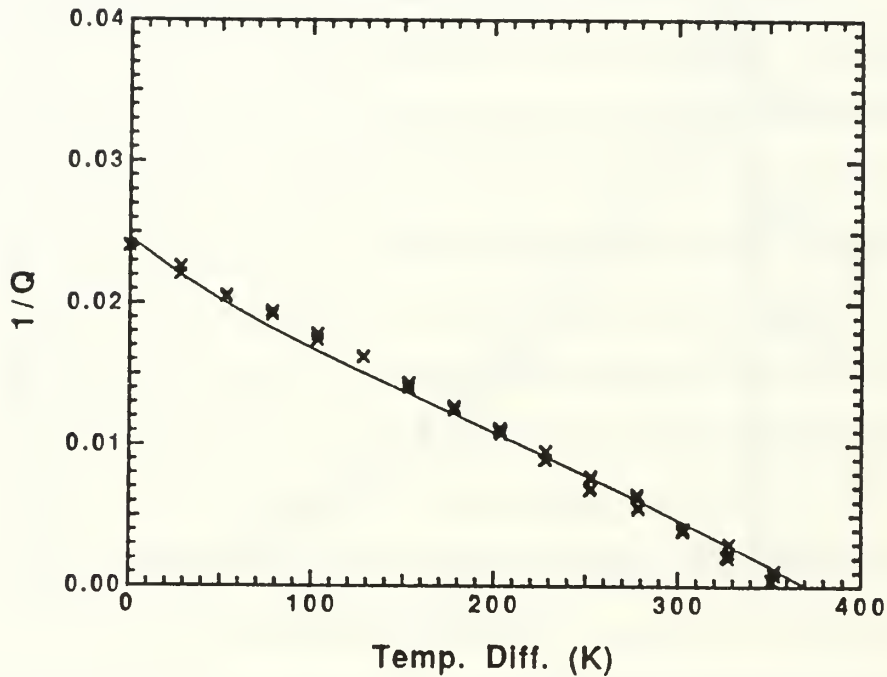


Figure 3. Graph of  $1/Q$  vs the temperature difference across the prime mover stack. The symbols represent the data, while the line represents the results of the calculations. The prime mover is filled with helium at a mean pressure of 500 kPa.

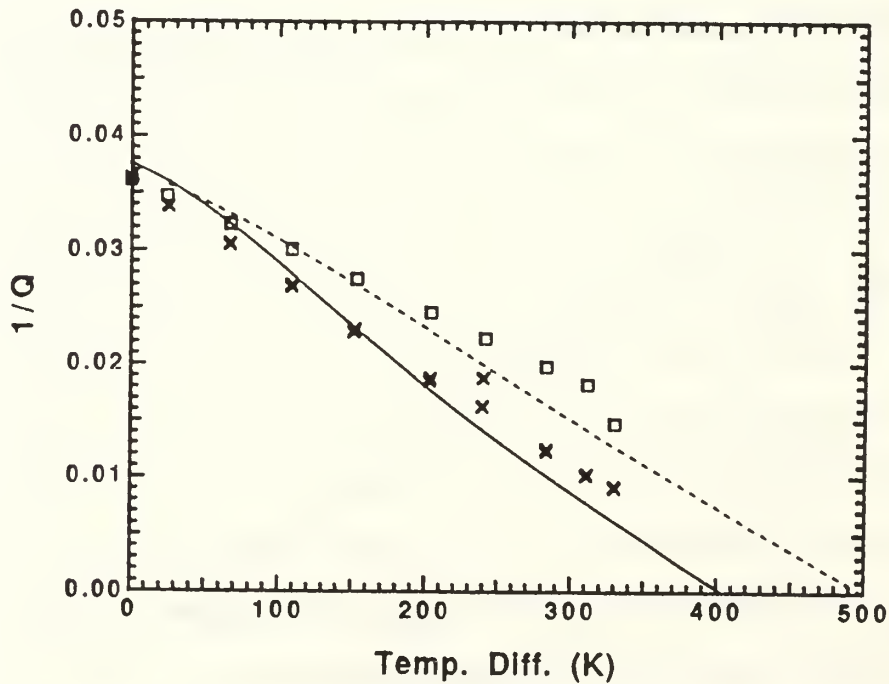


Figure 4. Graph of  $1/Q$  vs the temperature difference across the prime mover stack for the second and third longitudinal modes. The  $\times$ 's and solid line correspond to the second mode, while the open squares and dashed line correspond to the third. The prime mover is filled with helium at a mean pressure of 170 kPa.

### 3. Development of a Non-Boundary Layer, Non-Short Stack Model for the Power Output of a Prime Mover

Although our porous medium approach to prime movers offers decent agreement between measured and predicted quality factors, there is room for improvement. Therefore, we have pursued a different technique, described at length by Swift,<sup>7, 8</sup> to our prime mover data. The foundation of this technique is the calculation of the acoustic power generated by a differential element of prime mover surface area. Although the general technique is described by Swift, we use an expression for the power output not limited to either the small boundary layer or short stack approximations.<sup>9</sup> This expression is previously unpublished. In the calculations we take into consideration the temperature dependence of the thermophysical properties of both the gas and stack material.

The results of the analysis are shown in Figs. 5-8, which correspond to the same data as presented in Figs. 1-4, respectively. These results represent some of the first comparisons between Swift's theoretical approach and experimental measurements. Comparing Fig. 1 to Fig. 4, it is evident that the present technique provides a much better fit to the 170 kPa data. However, the two techniques do more-or-less equally well at 376 and 500 kPa and for the second and third modes at 170 kPa. There is a tendency for the present technique to under predict the attenuation at zero temperature difference.

Our analysis provides good overall prediction of the performance of a prime mover below onset. However, the true test is predicting the performance above onset. There are several significant differences between prime movers above and below onset. Most obvious is that the acoustic amplitudes above onset are quite large. Ratios of acoustic pressure amplitude to mean gas pressure of 1 - 10% are common. Yet, our analysis is based on linear acoustics. Beyond the theoretical

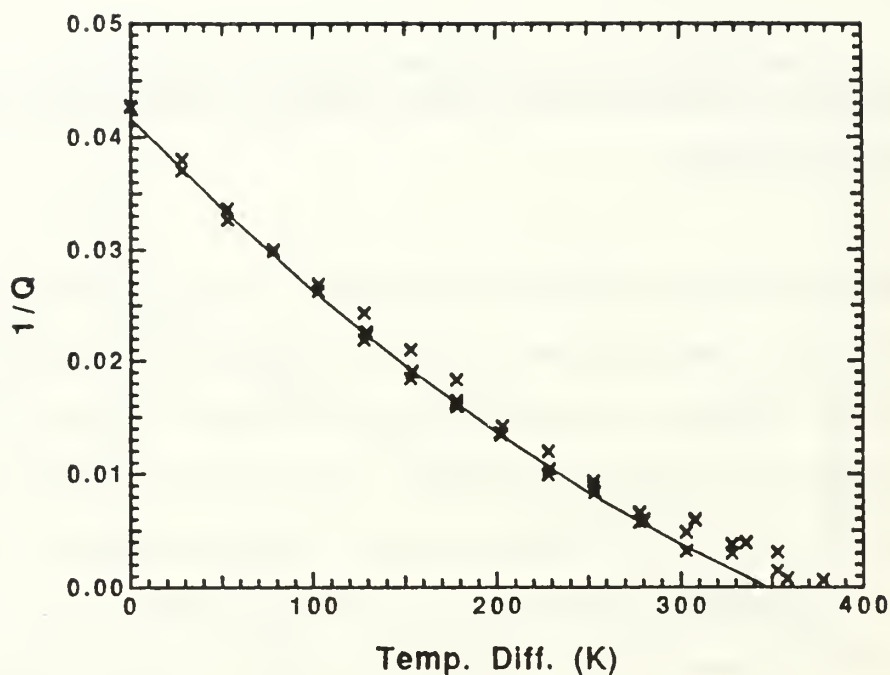


Figure 5. Graph of  $1/Q$  vs the temperature difference across the prime mover stack. The line represents the results of the calculations based on Swift's theoretical approach. The data are the same as presented in Fig. 1; the prime mover is filled with helium at a mean pressure of 170 kPa.

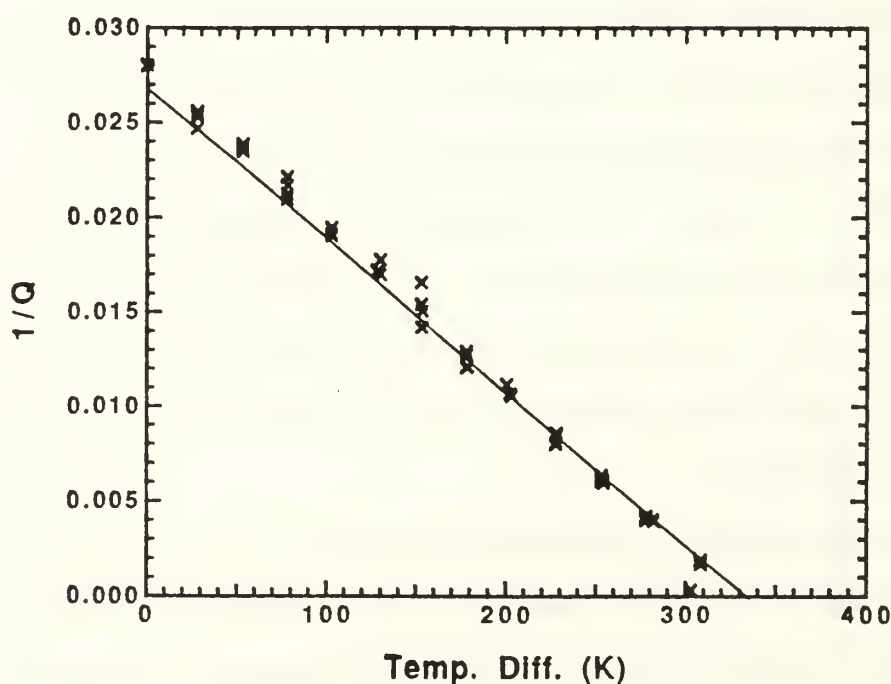


Figure 6. Graph of  $1/Q$  vs the temperature difference across the prime mover stack. The line represents the results of the calculations based on Swift's theoretical approach. The data are the same as presented in Fig. 2; the prime mover is filled with helium at a mean pressure of 376 kPa.

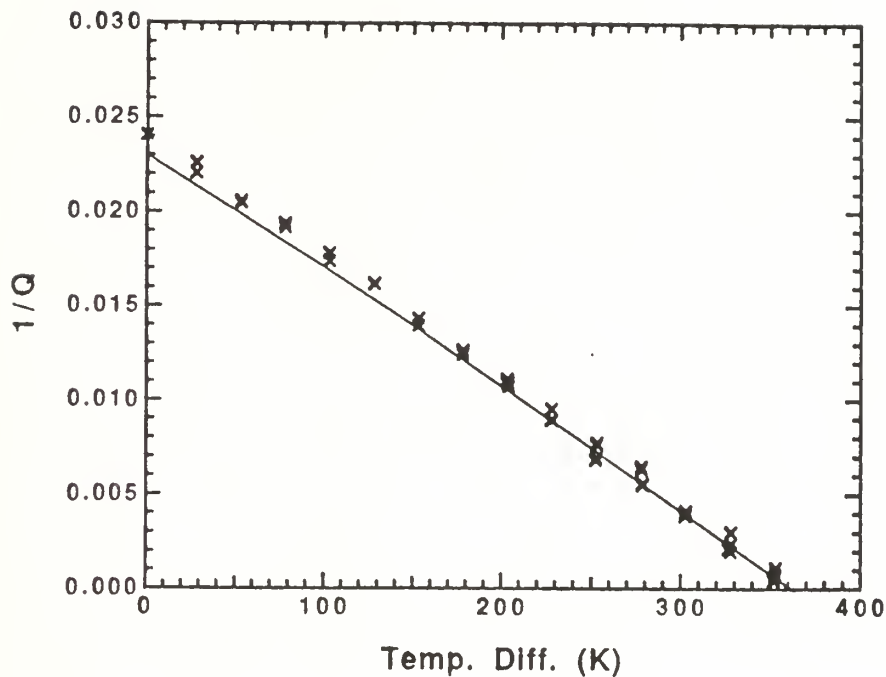


Figure 7. Graph of  $1/Q$  vs the temperature difference across the prime mover stack. The line represents the results of the calculations based on Swift's theoretical approach. The data are the same as presented in Fig. 3; the prime mover is filled with helium at a mean pressure of 500 kPa.

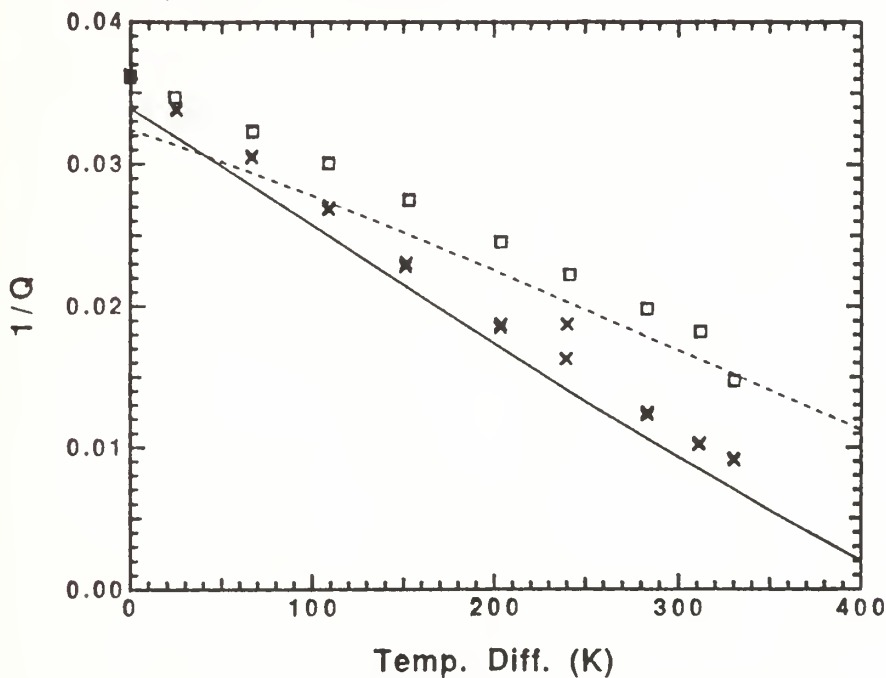


Figure 8. Graph of  $1/Q$  vs the temperature difference across the prime mover stack for the second and third longitudinal modes showing the results of the calculations based on Swift's theoretical approach.. The  $\times$ 's and solid line correspond to the second mode, while the open squares and dashed line correspond to the third. The data are the same as presented in Fig. 4; the prime mover is filled with helium at a mean pressure of 170 kPa.



complications added by introducing nonlinear effects, there are a number of experimental complications. For instance, the acoustic displacement amplitudes approach the length of the heat exchangers. Also, because of the large transport of heat, there is no assurance that the temperature gradient along the prime mover stack will be uniform.

The next logical step in this research is to investigate prime movers above onset, but still in the linear acoustics regime. This study is discussed in the next section.

#### 4. Study of the Transition to Steady State of a Prime Mover Above Onset

The natural progression of our investigations of prime movers below the onset of self-oscillation is to study the transition to steady state oscillation above onset. This work has been initiated in FY 1991. The below onset work consists of determining the net attenuation coefficient of a prime mover as a function of applied temperature gradient. The attenuation coefficient is determined from the frequency response. The goal of the above onset work is, also, to determine the net attenuation coefficient as a function of applied temperature gradient. Above onset, the attenuation (gain?) coefficient can be determined from the rise time of the acoustic oscillations. However, above onset the rise time is time dependent. It is small until some mechanism sets in to establish steady state, at which point it is infinite. Wheatley, et al made similar measurements,<sup>10</sup> although they were of a preliminary nature and little quantitative analysis was performed.

Our measurements are made in a prime mover fitted with a butterfly valve. With the valve closed the temperature gradient across the prime mover stack can be raised above the critical value required for onset without oscillations starting. When the valve is suddenly opened, the prime mover goes into self-oscillation and the acoustic amplitude begins to build up. Finally, the build-up ceases and steady

state is reached.

We are interested in three regions of the build-up of the acoustic oscillations. First, in the early stages of the build-up the amplitudes are low. From our past work, we expect that measurements made in this region should agree fairly well with predictions and the rise time to be constant. The second region of interest is the part of the build-up where the rise time begins to increase, deviating from its initial value. Knowing at what acoustic amplitude the rise time starts to deviate from its initial value should give some insight into what mechanisms cause this deviation. Finally, we are interested in the energy balance at steady state. In other words, we want to make sure that we can account for the dissipation of all the energy supplied by the prime mover. At this point we are investigating the low amplitude region.<sup>11</sup> The rise time of the oscillations is measured as a function of the temperature gradient and mean gas pressure in the prime mover. The results are analyzing using the technique based on Swift's approach discussed in Section 2.

We have found that soon after the oscillations begin harmonics start to appear in the spectrum of the waveform and the rise time deviates from its initial value. This behavior is indicated in Fig. 9 which shows a plot of the envelope of the signal amplitude (solid line) as a function of time. In this data record, harmonics began to appear in the spectrum after approximately 0.4 s. The dashed line is a least squares fit to the first 0.4 s of the data record. The two lines deviate significantly in the later portions of the record. Figure 10 shows the logarithm of the amplitude as a function of time. As a result of the observations we have limited our initial investigations to measuring the initial rise time of the oscillations, before the spectrum shows any significant harmonic content. Aside from this, these observations have taught us that harmonic generation plays a significant role in the transition to steady state.

Results of rise time measurements for a helium filled prime mover are shown in Figs. 11-14. To be consistent with the presentation of the data acquired below onset, the rise time has been converted to  $1/Q$ . Three points of comparison are

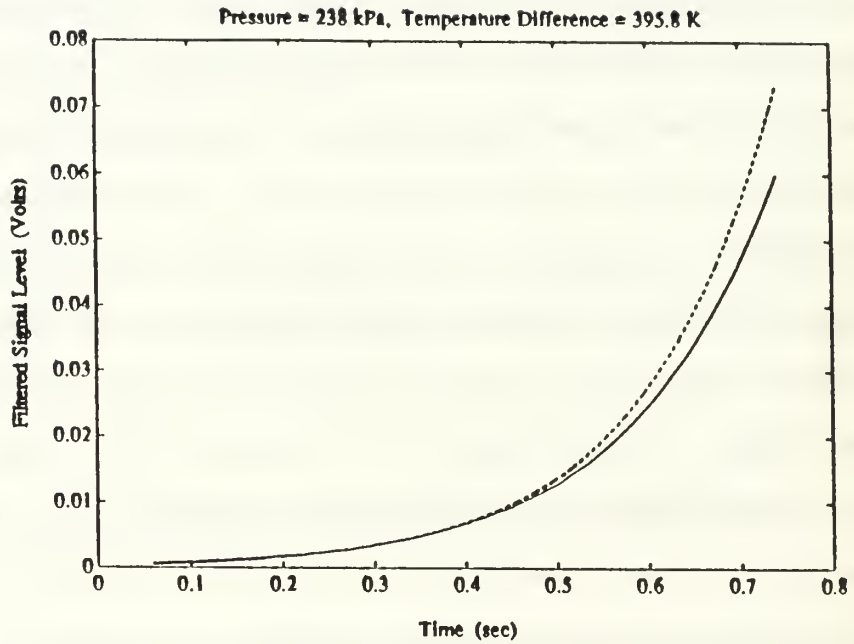


Figure 9. Graph of the envelope of the signal amplitude (solid line) as a function of time. The dashed line is a least squares fit to the first 0.4 s of the data record.

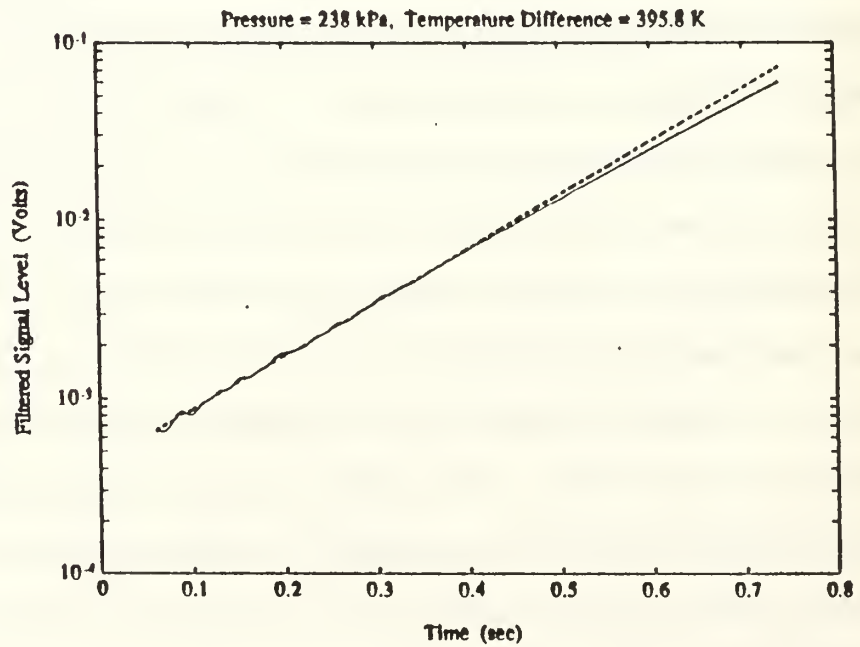


Figure 10. Graph showing the logarithm of the envelope of the signal amplitude as a function of time.

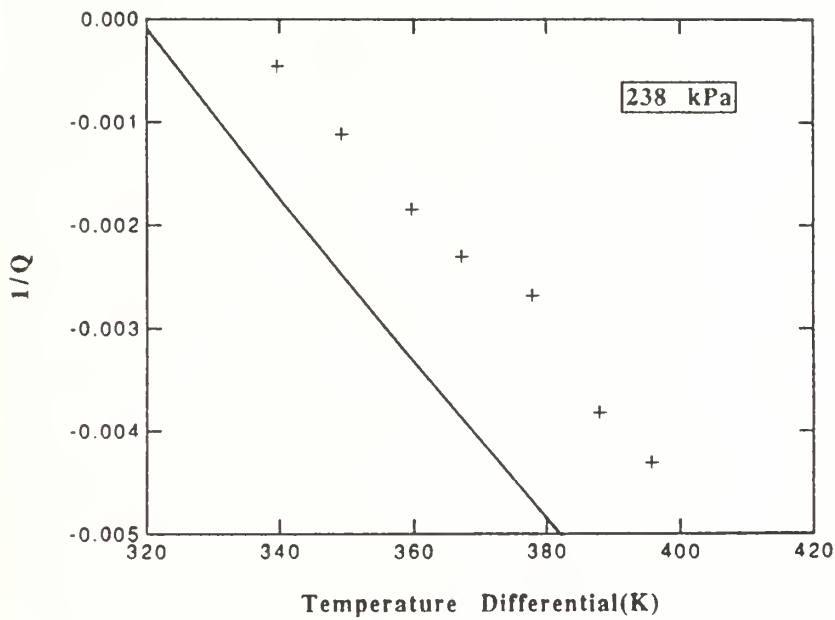


Figure 11. Data obtained for 238 kPa plotted as a function of the temperature difference across the stack. The solid line is the theoretical result.

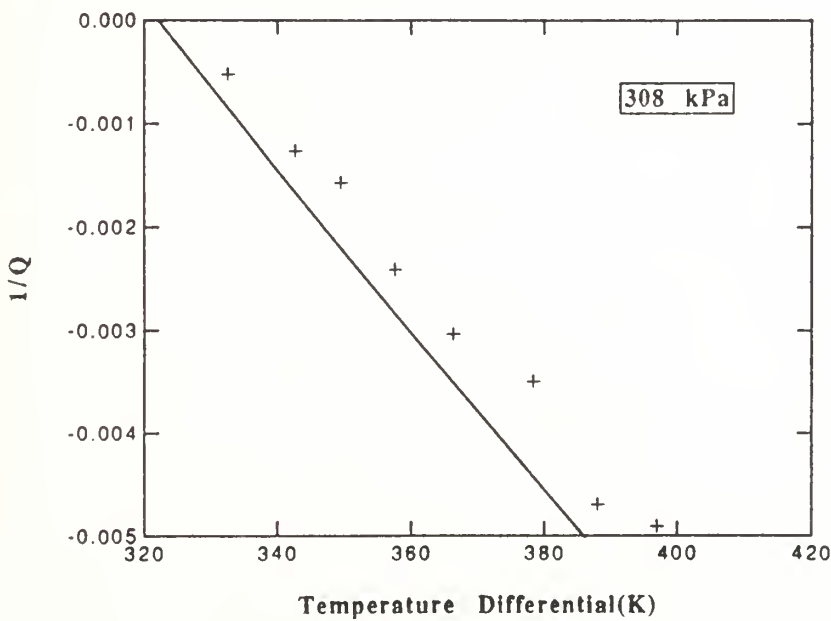


Figure 12. Data obtained for 308 kPa plotted as a function of the temperature difference across the stack. The solid line is the theoretical result.

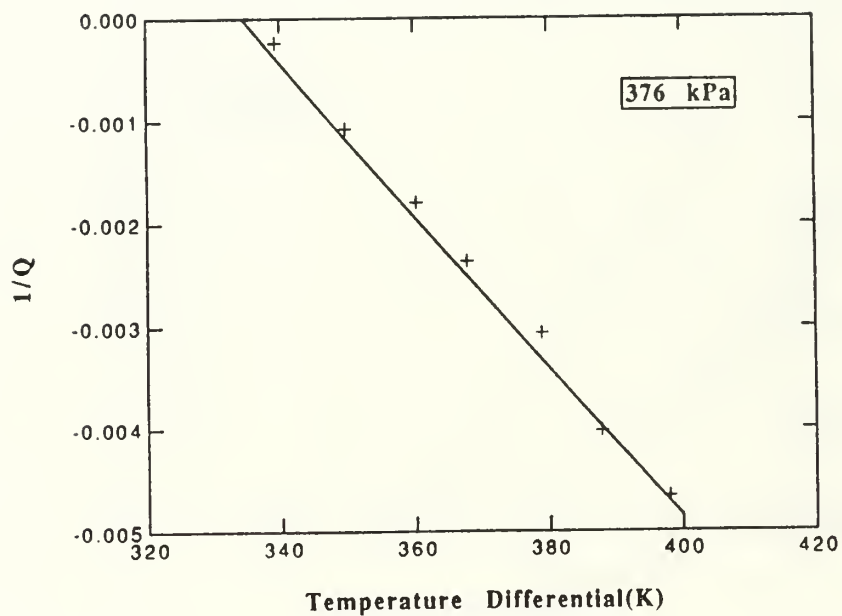


Figure 13. Data obtained for 376 kPa plotted as a function of the temperature difference across the stack. The solid line is the theoretical result.

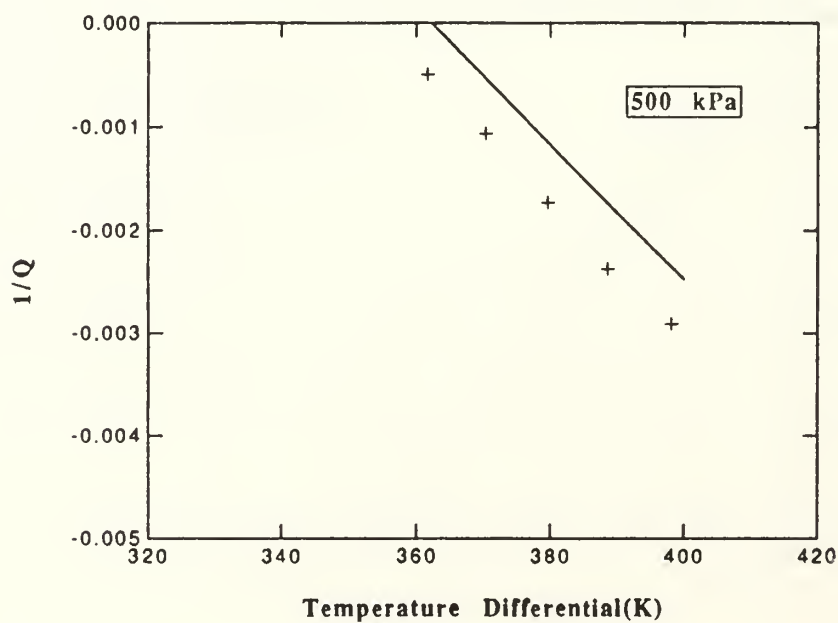


Figure 14. Data obtained for 500 kPa plotted as a function of the temperature difference across the stack. The solid line is the theoretical result.



evident. First, considering that there are no adjustable parameters in the model, the overall agreement is good, especially at the higher pressures. Second, the agreement between the predicted and measured onset temperatures, where  $1/Q = 0$ , for the various mean pressures is inconsistent. The third point of comparison is that the slopes of the predicted and measured results are quite close. This point is illustrated in Figs. 15-18. The predicted and experimental results presented in Figs. 11-14 were extrapolated to find the temperature difference at onset. The results are replotted in Figs. 15-18 as a function of the number of degrees above the extrapolated onset. In other words, the data and theory have been forced to fit at onset. As is evident, the agreement is very good at the higher pressures but not quite as good at the lower pressures. Recall that the agreement below onset followed the same trend. The reason for this tendency is unknown. However, one possible cause has to do with imperfections in the stack construction. At the lowest pressure, the plate spacing to penetration depth ratio is on the order of two or less, which is just at the critical value. The heat transport occurs in a region about a penetration depth away from each plate. Therefore, imperfections in the plate spacing could alter the volume of gas available for heat transport significantly at these pressures. However, these imperfections would have less effect at higher pressures where the plate spacing to penetration depth ratio is larger.

The accurate prediction of the slope is more important than an accurate prediction of the onset temperature. The inability to predict the precise onset temperature may be tied to errors in predicting the attenuation of the entire prime mover at zero temperature difference. Whereas the ability to predict the slope well indicates that the model is able to predict the change in power output with applied temperature difference well. In other words our understanding of the stack performance and how that performance changes with changing temperature gradient is good. We are currently taking data with the prime mover filled with argon in attempt to further investigate the nature of the discrepancies.

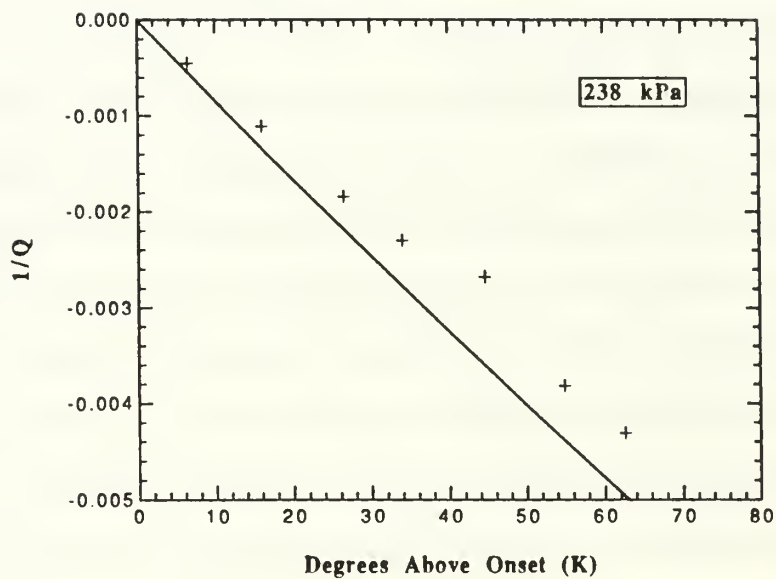


Figure 15. Data obtained for 238 kPa plotted as a function of the number of degrees above the extrapolated onset.

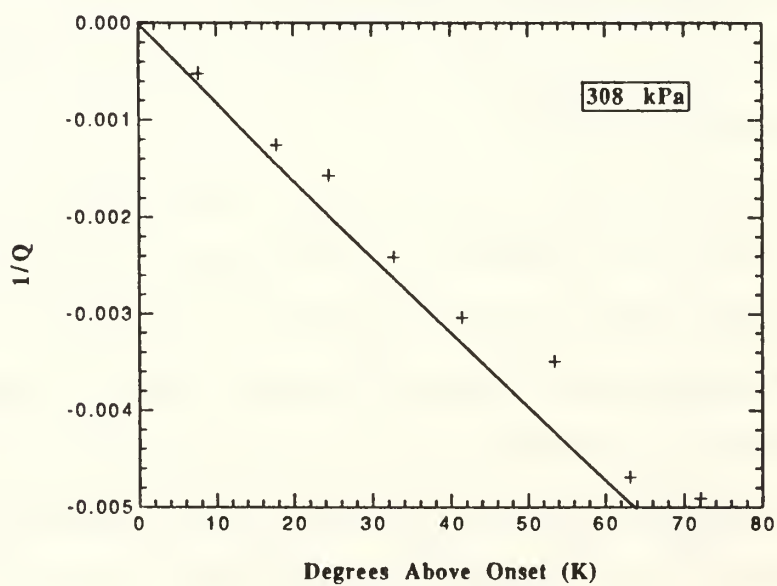


Figure 16. Data obtained for 308 kPa plotted as a function of the number of degrees above the extrapolated onset.

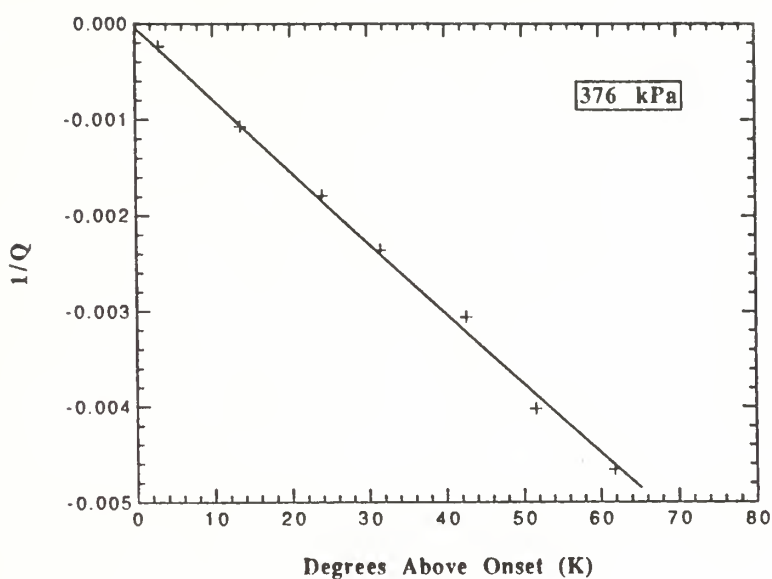


Figure 17. Data obtained for 376 kPa plotted as a function of the number of degrees above the extrapolated onset.

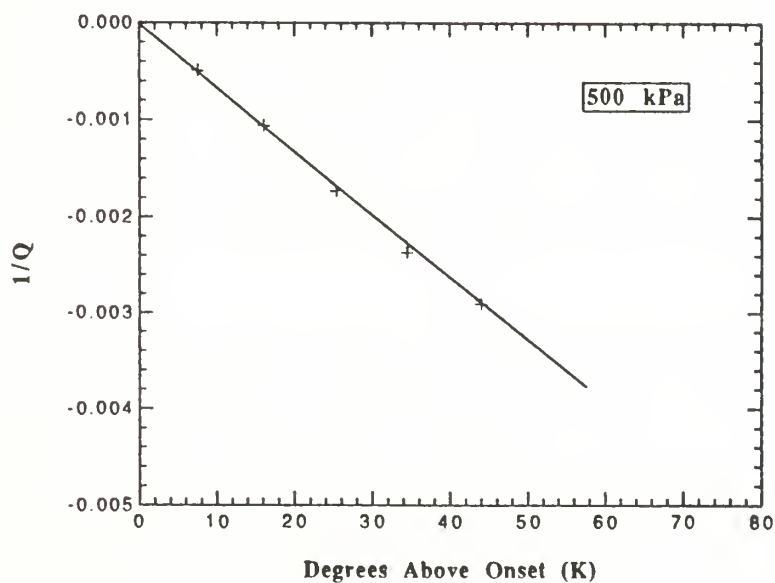


Figure 18. Data obtained for 500 kPa plotted as a function of the number of degrees above the extrapolated onset.

## 5. Study of Energy Distribution and Dissipation in Finite Amplitude Standing Waves

In addition to the harmonic generation discussed in Section 4, we have previously observed nonlinear effects in our prime mover above onset.<sup>12,13</sup> These effects are manifested in the generation of harmonics of the fundamental frequency, thus taking energy out of the fundamental mode. Because typical standing wave thermoacoustic engines are designed to operate optimally at the fundamental frequency, the transfer of energy to higher harmonics represents a parasitic loss. Some questions arise. How much of the input energy is lost from the fundamental mode? Is there a way to prevent this loss? Some of these questions can be answered by understanding the steady state energy balance in the prime mover. As a first step toward understanding energy balance in the prime mover, we have begun an investigation of the energy balance in a simpler system - a rigid tube.

Our efforts in this area began with the observation that the waveforms observed in our prime mover are very similar to those observed by Coppens and Sanders.<sup>14</sup> Their system consisted of a rigid tube driven with a piston source at one end. We have created a similar setup (using their original tube and source) and made measurements of the steady state energy distribution in finite amplitude standing waves.

The first measurements were made on an empty tube. The tube was driven at its fundamental resonance frequency. The steady state power input to the tube by the piston was computed from measurements of the acceleration of the piston and the acoustic pressure amplitude at the piston location. This power was compared to the steady state acoustic power dissipated by thermal and viscous losses at the tube walls by the fundamental and higher harmonics. The results are shown in Figs. 19 and 20. In these figures,  $\dot{E}_n$  represents the power dissipated by the  $n^{\text{th}}$  harmonic

(where  $n = 1$  corresponds to the fundamental).  $\dot{E}_{\text{input}}$  is the total power input to the tube by the piston. It can be seen that at the highest drive levels, only 85% of the power remains in the fundamental. Conversely, 15% of the power delivered at the fundamental is dissipated by higher harmonics, the result of nonlinear effects. Figure 21 shows the ratio of the total dissipated power  $\dot{E} = \dot{E}_1 + \dot{E}_2 + \dots$  to  $\dot{E}_{\text{input}}$ . The fact that this ratio is very close to unity implies that our system behaves as expected. Figure 22 shows a typical waveform and spectrum of the acoustic pressure at the highest drive levels. Notice the severe distortion of the waveform and the associated rich spectral content.

The next set of measurements was made on an obstructed tube. The obstruction, shown in Fig. 23, is an insert located at the midpoint of the original empty tube. As seen from Table 1, the obstruction changes the resonance frequencies of the tube so that the harmonics of the fundamental (drive) frequency no longer match the overtones of the tube. It detunes the resonator. The same measurements were repeated as with the empty tube. Figure 24 shows a typical waveform and spectrum at the same drive levels as shown in Fig. 22. (Note that the time and frequency spans are different from those in Fig. 22.) The waveform is much less distorted. This can be seen visually or by the relatively few numbers of harmonics in the spectrum. Clearly, the detuning cleans up the waveform. But what effect does this have on the energy distribution? Do we still know where all the energy is going?

The second harmonic of the pressure waveform is more than 35 dB below the fundamental amplitude and so accounts for less than a few hundredths of a percent of the total acoustic energy. Therefore,  $\dot{E}$  can be approximated by  $\dot{E}_1$ . Figure 24 shows  $\dot{E}/\dot{E}_{\text{input}}$  for the obstructed tube. There is a systematic decrease in the ratio from approximately unity to 0.93 as the drive amplitude increases. For the reasons given at the beginning of the paragraph, this energy does not show up in other acoustic modes. Where the unaccounted for energy goes is not known. There may be



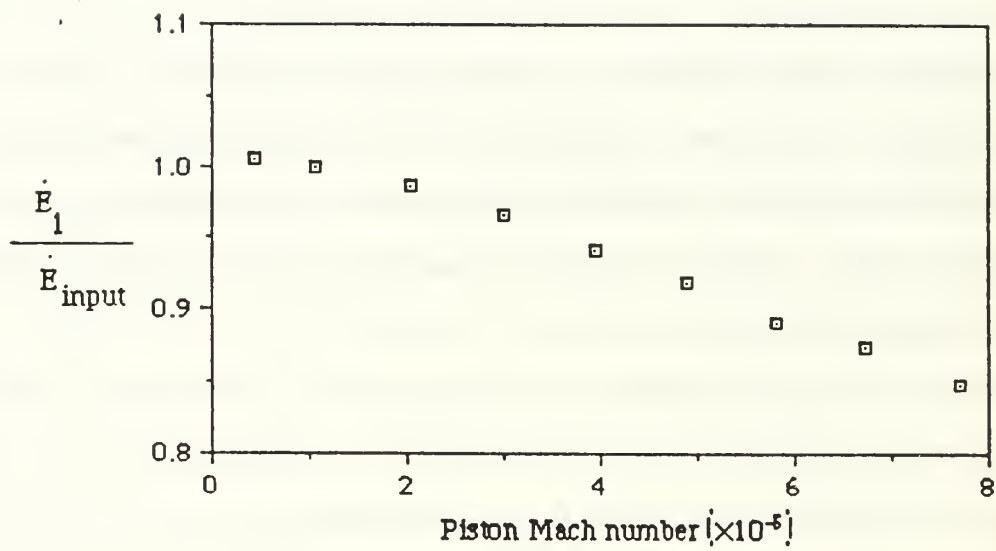


Figure 19. Measured ratio of  $\dot{E}_1 / \dot{E}_{input}$  as a function of the piston Mach number for the empty tube.

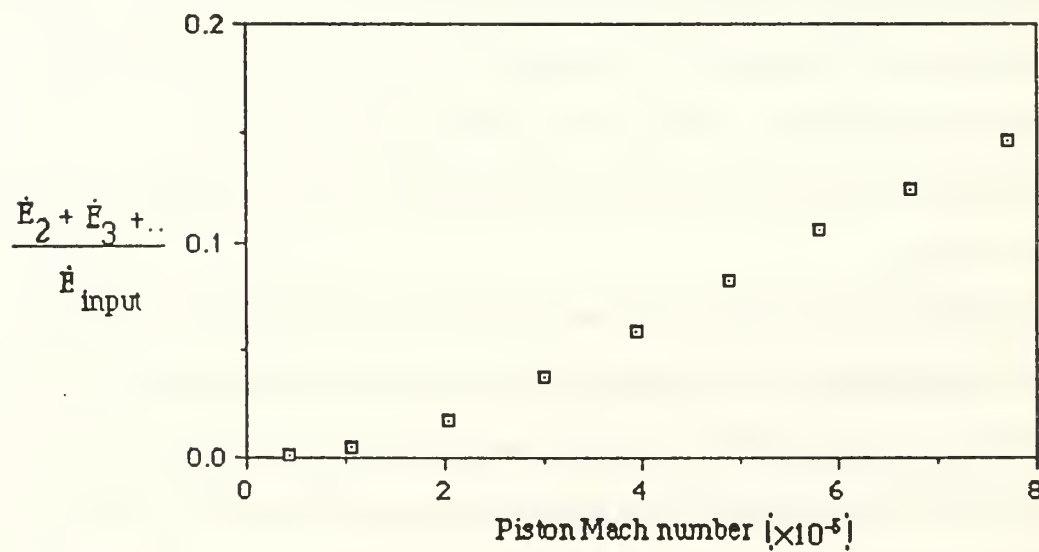


Figure 20. Measured ratio of  $\dot{E}_2 + \dot{E}_3 + \dots / \dot{E}_{input}$  as a function of the piston Mach number for the empty tube.

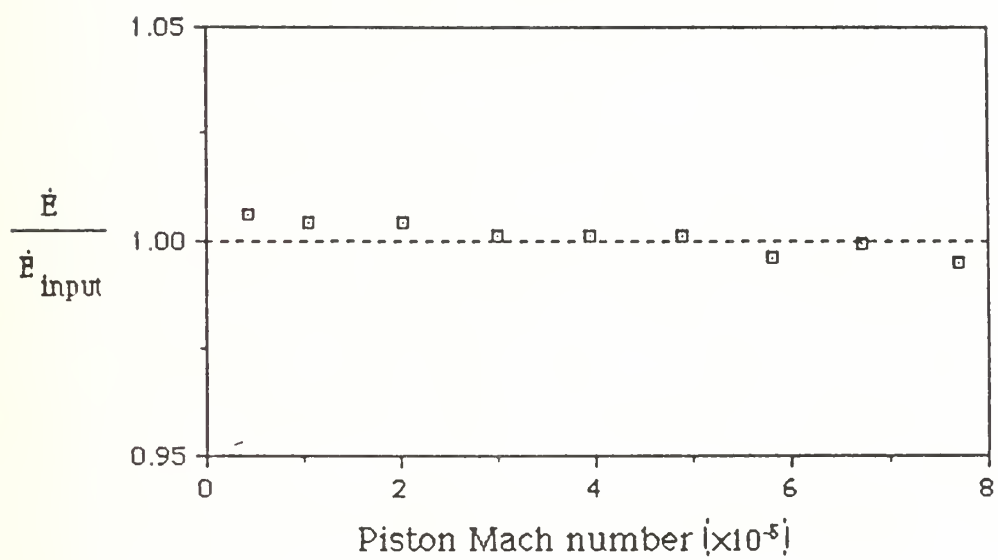


Figure 21. Measured ratio of  $\dot{E}/\dot{E}_{input}$  as a function of the piston Mach number for the empty tube.

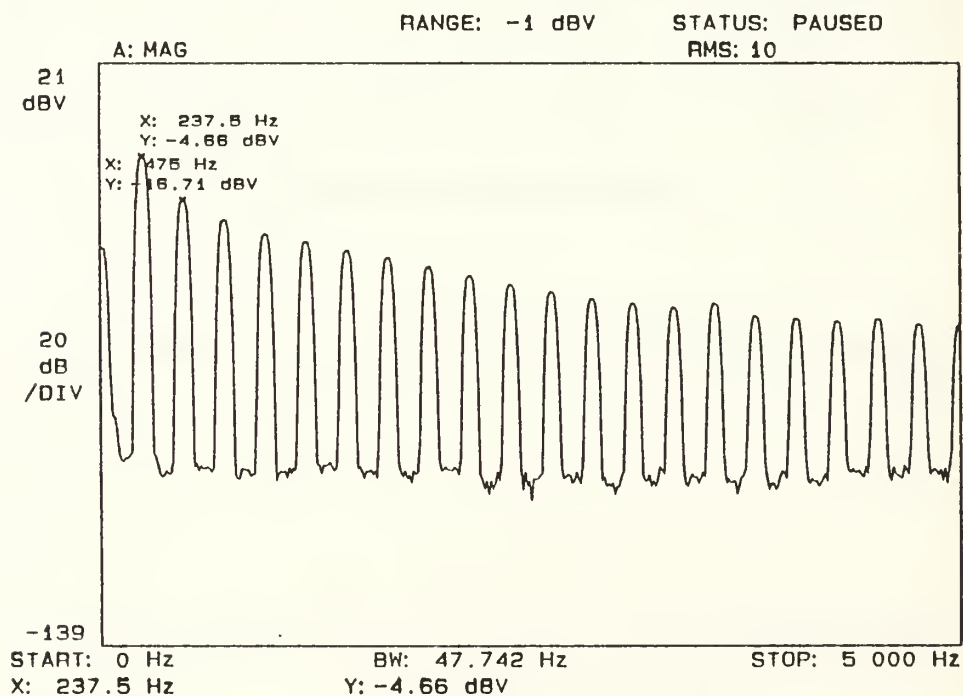
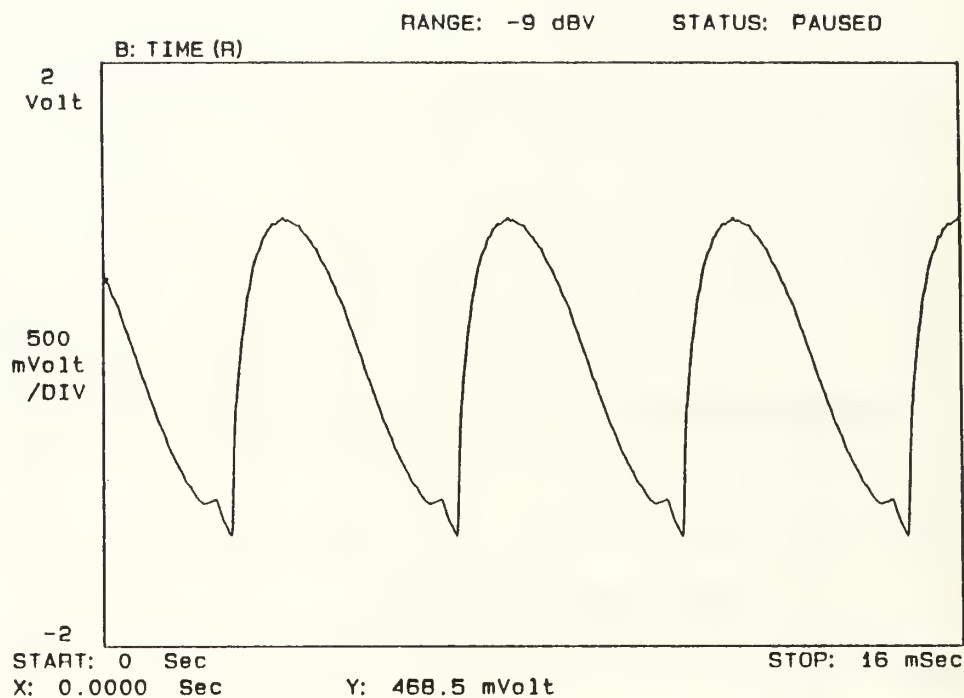


Figure 22. A typical waveform (top) and spectrum (bottom) of the acoustic pressure at the highest drive levels in the empty tube.

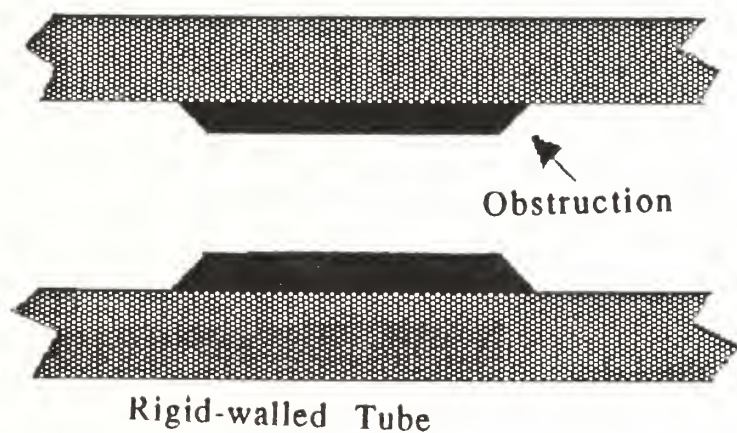


Figure 23. Illustration of the obstruction that is inserted into the empty tube.

Mode	Empty Tube		Obstructed Tube	
	$f_n$ (Hz)	$f_n/f_1$	$f_n$ (Hz)	$f_n/f_1$
1	238	1.000	227	1.000
2	477	2.004	487	2.144
3	715	3.004	686	3.019
4	955	4.013	974	4.289
5	1194	5.017	1153	5.077

Table 1. Measured resonance frequencies for the first five modes of the empty and obstructed tubes.

turbulence generated at the tube/obstruction transitions. Also, there are cavities between the inner tube wall and the outer obstruction wall that may be contributing to the problem. We are in the process of redesigning the resonator to eliminate these cavities.

In spite of the systematic decrease in the ratio, the results with the obstructed tube clearly are better than the 15% energy loss from the empty tube. The results suggest that resonators with nearly harmonic overtones are to be avoided in thermoacoustics work. This conclusion may seem painfully obvious, but now we have some ideas of the magnitude of the problem. There is also probably something to learn from the systematic decrease in  $\dot{E}/\dot{E}_{\text{input}}$  for the obstructed tube. Finally, we are able to account for the energy balance in finite amplitude standing waves (in empty tubes at least). This ability will be applied to steady state oscillations in prime movers in FY 1992.



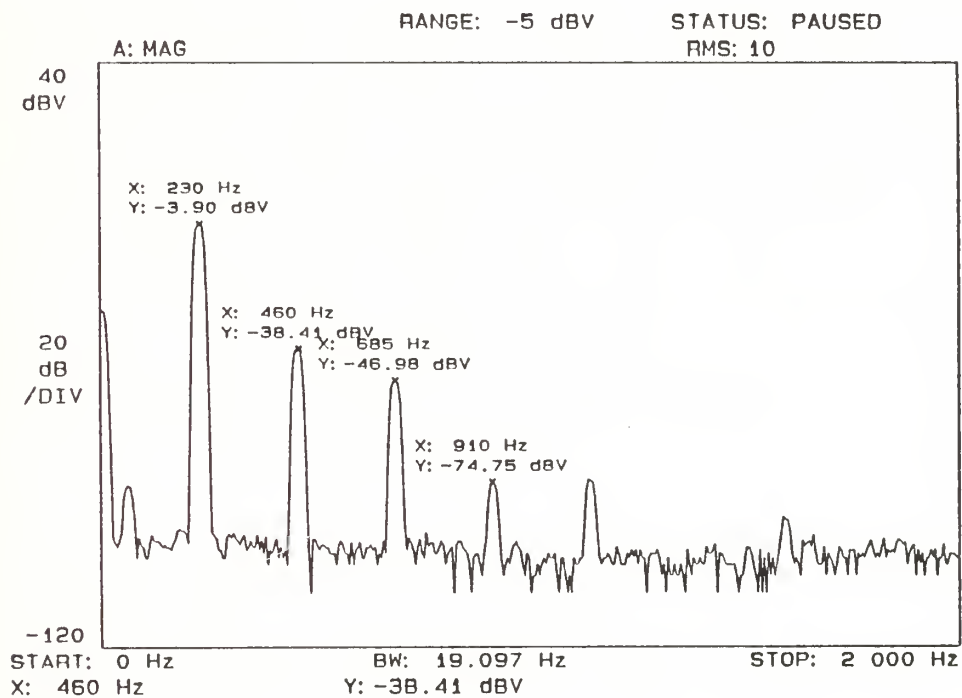
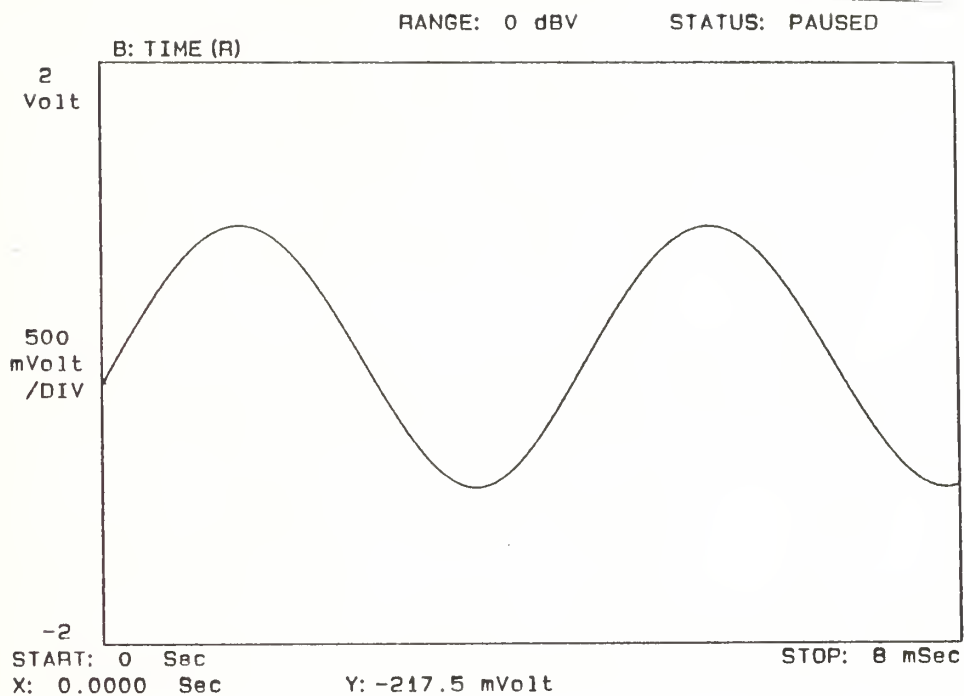


Figure 24. A typical waveform (top) and spectrum (bottom) of the acoustic pressure at the highest drive levels in the obstructed tube.

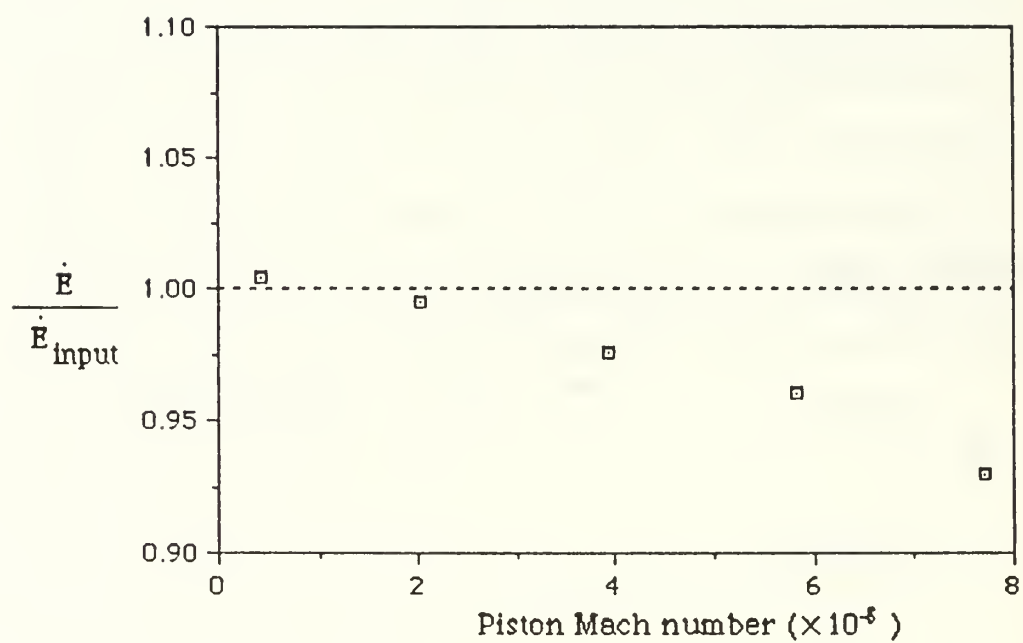


Figure 25. Measured ratio of  $\dot{E}/\dot{E}_{input}$  as a function of the piston Mach number for the obstructed tube.

## REFERENCES

1. Anthony A. Atchley, Thomas J. Hofler, Michael L. Muzzerall, M. David Kite, and Ao, Chia-ning, "Acoustically generated temperature gradients in short plates," J. Acoust. Soc. Am. 88, 251-263, (1990).
2. Anthony A. Atchley and Thomas J. Hofler, "Annual summary of basic research in thermoacoustic heat transport: 1990," Naval Postgraduate School Report Number NPS PH-91-002PR, 30 pages, October, 1990.
3. W. H. Liu, "Investigation of Edge Effects in Thermoacoustic Couple Measurements," Master's Thesis, Naval Postgraduate School, Dec. 1990.
4. A. A. Atchley, H. E. Bass, T. J. Hofler and H. T. Lin, "Study of a thermoacoustic prime mover below the onset of self-oscillation," Accepted for publication J. Acoust. Soc. Am. (Expected publication date January, 1992).
5. W. Pat Arnott, Henry E. Bass and Richard Raspet, "General formulation of thermoacoustics for stacks having arbitrarily-shaped pore cross sections," Submitted to J. Acoust. Soc. Am. (1991).
6. W. Pat Arnott, Richard Raspet and Henry E. Bass, "Complex eigenfrequency analysis of thermoacoustic heat engines," J. Acoust. Soc. Am. 89, 2007(A), (1991).
7. G. W. Swift, "Thermoacoustic engines," J. Acoust. Soc. Am. 84 (4), 1145 - 1180 (1988).

8. G. W. Swift, A. Migliori, T. Hofler and John Wheatley, "Theory and calculations for an intrinsically irreversible acoustic prime mover using liquid sodium as a primary working fluid," J. Acoust. Soc. Am. 78 (2), 767 - 781 (1985).
9. Anthony A. Atchley, "The power output of a thermoacoustic prime mover below onset of self-oscillation," to be submitted to J. Acoust. Soc. Am. (1991).
10. John Wheatley, T. Hofler, G. W. Swift, and A. Migliori, "Understanding some simple phenomena in thermoacoustics with applications to acoustical heat engines," Am. J. Phys. 53, 147 - 162 (1985).
11. Earl C. Bowers, "Investigation of a heat driven thermoacoustic prime mover above the onset of self-oscillation," Master's Thesis, Naval Postgraduate School, September 1991.
12. H. T. Lin, "Investigation of a Heat Driven Thermoacoustic Prime Mover," Master's Thesis, Naval Postgraduate School, December 1989.
13. A. A. Atchley, H. E. Bass and T. J. Hofler, "Development of nonlinear waves in a thermoacoustic prime mover," Frontiers of Nonlinear Acoustics 12th ISNA, edited M. F. Hamilton and D. T. Blackstock (Elsevier Applied Science, New York, 1990), pp. 603-608.
14. A.B. Coppens and J.V. Sanders, "Finite-amplitude standing waves in rigid-walled tubes," J. Acoust. Soc. Am. 43(3), 516-529 (1968).

OFFICE OF NAVAL RESEARCH  
PUBLICATIONS / PATENTS / PRESENTATIONS / HONORS REPORT  
FOR

1 OCTOBER 1990 through 30 SEPTEMBER 1991

\*\*\*\*\*

CONTRACT N00014-91WR24003

R&T NO. 4126949

TITLE OF CONTRACT: BASIC RESEARCH IN THERMOACOUSTIC HEAT  
TRANSPORT

NAME OF PRINCIPAL INVESTIGATOR: ANTHONY A. ATCHLEY

NAME OF ORGANIZATION: PHYSICS DEPARTMENT  
NAVAL POSTGRADUATE SCHOOL

ADDRESS OF ORGANIZATION: MONTEREY, CA 93943

\*\*\*\*\*

Reproduction in whole, or part, is permitted for any purpose of the United States Government.

This document has been approved for public release and sale; its distribution is unlimited.

PAPERS SUBMITTED TO REFEREED JOURNALS  
(Not yet published.)

Anthony A. Atchley, Henry E. Bass, Thomas, J. Hofler and Hsiao-Tseng Lin,  
"Study of a thermoacoustic prime mover below onset of self-oscillation,"  
Accepted for publication in J. Acoust. Soc. Am.

PAPERS PUBLISHED IN REFEREED JOURNALS

Anthony A. Atchley, "Report of the 8th F. V. Hunt Postdoctoral Fellow (1985-1986)," J. Acoust. Soc. Am. 88, 2895(L), (1990).

PAPERS PUBLISHED IN NON-REFEREED JOURNALS

N/A

TECHNICAL REPORTS PUBLISHED

N/A

BOOKS (AND SECTIONS THEREOF) SUBMITTED FOR PUBLICATION

Henry E. Bass, J. Brian Fowlkes and Anthony A. Atchley, "Ultrasonics,"  
Encyclopedia of Science and Technology 6th Edition (McGraw-Hill, New York,  
1991?).



BOOKS (AND SECTIONS THEREOF) PUBLISHED

N/A

PATENTS FILED

N/A

PATENTS GRANTED

N/A

INVITED PRESENTATIONS AT TOPICAL OR  
SCIENTIFIC/TECHNICAL SOCIETY CONFERENCES

Anthony A. Atchley, "The past, present and future of acoustic cavitation nucleation," J. Acoust. Soc. Am. 89, No. 4, Pt. 2, 1884(A) (1991).

Henry E. Bass, Anthony A. Atchley and Thomas J. Hofler, "Study of a parallel plate thermoacoustic prime mover," J. Acoust. Soc. Am. 88, Suppl. 1, S95(A) (1990).

CONTRIBUTED PRESENTATIONS AT TOPICAL OR  
SCIENTIFIC/TECHNICAL SOCIETY CONFERENCES

N/A

## HONORS/AWARDS/PRIZES

NPS Faculty Performance Award 1990

Chairman, Committee on Education in Acoustics, Acoustical Society of America

## GRADUATE STUDENTS SUPPORTED UNDER CONTRACT FOR YEAR ENDING 30 SEPTEMBER 1991

No support for graduate students is required at the Naval Postgraduate School.

## POSTDOCTORALS SUPPORTED UNDER CONTRACT FOR YEAR ENDING 30 SEPTEMBER 1991

Dr. Felipe Gaitan

## DISTRIBUTION LIST

Director Defense Advanced Research Projects Agency Attn: Technical Library, TIO 1400 Wilson Blvd. Arlington, VA 22209-2309	1 copy
Office of Naval Research Physics Division Office (Code 1112) 800 North Quincy Street Arlington, VA 22217-5000	2 copies
Office of Naval Research Director, Technology (Code 02) 800 North Quincy Street Arlington, VA 22217-5000	1 copy
Naval Research Laboratory Department of the Navy (Code 2625) Attn: Technical Library Washington, DC 20375-5000	1 copy
Office of the Director of Defense Research and Engineering Information Office Library Branch The Pentagon, Rm. 3E 1006 Washington, DC 20310	1 copy
U.S. Army Research Office Box 12211 Research Triangle Park North Carolina 27709-2211	2 copies
Defense Technical Information Center Cameron Station Alexandria, VA 22314	2 copies
Director National Bureau of Standards Research Information Center Attn: Technical Library (Admin E-01) Gaithersburg, MD 20899	1 copy

Commander U. S. Army Belvoir Research, Development, and Engineering Center Attn: Technical Library (STRBE-BT) Fort Belvoir, VA 22060-5606	1 copy
ODDR&E Advisory Group on Electron Devices 210 Varick Street, 11th Floor New York, NY 10014-4877	1 copy
Air Force Office of Scientific Research Department of the Air Force Bolling AFB, DC 22209	1 copy
Air Force Weapons Laboratory Technical Library Kirkland Air Force Base Albuquerque, NM 87117	1 copy
Lawrence Livermore Laboratory Attn: Dr. W. K. Krupke University of California P. O. Box 808 Livermore, CA 94550	1 copy
Harry Diamond Laboratories Technical Library 2800 Powder Mill Road Adelphi, MD 20783	1 copy
Naval Weapons Center Technical Library (Code 753) China Lake, CA 93555	1 copy
Naval Underwater Systems Center Technical Center New London, CT 06320	1 copy
Commandant of the Marine Corps Scientific Advisor (Code RD-1) Washington, DC 20380	1 copy
Naval Ordnance Station Technical Library Indian Head, MD 20640	1 copy

Naval Postgraduate School Technical Library (Code 52) Monterey, CA 93943	2 copies
Naval Missile Center Technical Library (Code 5632.2) Point Mugo, CA 93010	2 copies
Naval Ordnance Station Technical Library Louisville, KY 40214	1 copy
Commanding Office Naval Ocean Research & Development Activity Technical Library NSTL Station, MS 39529	1 copy
Naval Oceans Systems Center Technical Library Silver Spring, MD 20910	1 copy
Naval Ship Research and Development Center Central Library (Codes L42 and L43) Bethesda, MD 20084	1 copy
Naval Avionics Facility Technical Library Indianapolis, IN 46218	1 copy
Director Research Administration (Code 81) Naval Postgraduate School Monterey, CA 93943	1 copy
Professor Anthony A. Atchley Physics Department (Code PH/Ay) Naval Postgraduate School Monterey, CA 93943	5 copies







DUDLEY KNOX LIBRARY



3 2768 00347382 8